

This is the peer reviewed version of: Lees J.M. and Burgoyne C.J. (1999)
"Experimental study of the influence of bond on the flexural behaviour of concrete
beams pre-tensioned with AFRPs" ACI Structural Journal v. 96(3) pp. 377-385.

Experimental Study of the Influence of Bond on the Flexural Behaviour of Concrete Beams Pre-tensioned with AFRPs

by J.M. Lees, C.J. Burgoyne

SYNOPSIS

An experimental program was formulated to investigate the flexural behaviour of concrete prestressed with aramid fibre reinforced plastic tendons (AFRPs). The particular focus was the influence of the bond between an AFRP tendon and concrete on the flexural response of a beam.

In the main test series pre-tensioned concrete beams were cast using either one of two types of AFRP tendons or steel tendons. The influence of bond was studied by testing beams with fully-bonded tendons, unbonded tendons or partially-bonded tendons. It was found that, although the fully-bonded beams had a high ultimate load capacity, only limited rotation occurred prior to failure. In contrast, large rotations were noted in the unbonded beams but the strengths of these members were significantly (25%) lower than those of the fully-bonded beams. The only beams that achieved both a high

rotation capacity and a high ultimate load capacity were the beams with partially-bonded tendons.

It is suggested that the use of partially-bonded tendons could provide the basis of a new design method for concrete beams prestressed with FRPs.

Key words : Prestressed concrete, flexure, bond, advanced composites, aramid, FRP, fibre reinforced plastics

INTRODUCTION

The social and financial costs associated with the repair of existing corrosion-damaged steel reinforced concrete infrastructure are high. In the UK, the Department of Transport has only recently lifted a 4 year ban on the use of grouted steel prestressing tendons. The ban had been imposed because of fears of the tendons corroding and the difficulties associated with the detection of this type of deterioration. The problems associated with steel corrosion are most severe in countries where road deicing salts are used extensively. The construction industry needs to seek alternatives to steel reinforcement; a potential solution is the use of fibre reinforced plastics (FRPs) as concrete reinforcement.

The term, *fibre reinforced plastics*, describes a group of materials composed of inorganic or organic fibres embedded in a resin matrix. FRPs are light-weight, strong, non-magnetic and, for the most part, non-corrodible. It is the last property which is particularly attractive to designers.

In the construction industry, the most commonly used FRPs are glass fibre reinforced plastics (GFRPs), carbon fibre reinforced plastics (CFRPs) and aramid fibre

reinforced plastics (AFRPs). Figure 1 shows typical stress-strain properties of these three materials and steel. The focus of the present study is AFRPs, but it is believed that the principles identified in the current work are applicable to all three types of FRP materials.

RESEARCH SIGNIFICANCE

Conventional flexural design methods for steel-prestressed concrete members are based on the assumption that the steel will yield prior to the failure of the beam. When the steel yields, large deflections ensue and inelastic energy is absorbed. The absorption of inelastic energy results in a *ductile* structure.

FRP materials are linearly elastic and do not yield. Hence the amount of plastic energy dissipated in an FRP system is much less than with a steel-prestressed system. As there is a high proportion of elastic energy in a structure with FRP reinforcement, it is essential that large rotations occur in these members to warn of pending failure.

The distinction between rotation capacity and ductility is important. The occurrence of large elastic rotations in a member prestressed with FRPs does not necessarily result in a ductile structure. Final failure due to rupture of the FRP tendons will be brittle and sudden, with large amounts of elastic energy being released. From a safety point of view, the necessity of a high rotation capacity in members with FRP tendons therefore becomes crucial.

The FRP industry had been producing tendons that were indented to look like reinforcing bars, and they were conducting tests to demonstrate the high bond capacities that could be achieved. Burgoyne¹ questioned the desirability of this approach. The

aim of the present study was to demonstrate the influence of the bond between the AFRP tendon and concrete on the rotation capacity of a concrete beam prestressed with AFRPs.

THE INFLUENCE OF BOND

Before cracking occurs, the strains in the concrete are small, and fairly uniform over the length of the beam, so the degree of bond has relatively little effect on the behaviour of the beam. However, once cracking occurs in the concrete, the amount of bond can have a significant effect.

Beams with fully-bonded tendons must have the same change in strain in both the tendon and the concrete, except at the crack locations where there must be some breakdown of bond on either side of the crack. If the tendon can yield (as for steel tendons) high bond stresses do not cause a problem; the tendon carries its yield load and can stretch plastically to maintain compatibility. However, if the tendon cannot yield (as for FRP tendons) it will snap as soon as the strain reaches a limiting value. The result will be a high moment capacity, since the tendon reaches its failure load, but limited rotation capacity.

With unbonded or external tendons, the tendon is free to slide relative to the concrete. The strain increase in the tendon due to the displacement is distributed fairly uniformly along the length of the tendon. Large rotations can be realised since the concrete can have a large strain at a few crack locations, while the tendon has a relatively low strain over its whole length. The corollary is that since the tendon's strain, and hence stress, are low, the moment capacity is reduced and the final failure is typically

due to premature concrete crushing at one of the crack locations.

The idea of partial bond is thus to obtain the best of both worlds. There should be sufficient bond to allow the tendon to achieve its full strength, but the amount of bond must be limited to ensure that the tendon can achieve high strains over a reasonable length before failure. Both a high ultimate load capacity and high rotation can then be achieved (see Figure 2).

In the current work, partial bonding was achieved in two ways; either by intermittently bonding sections of tendon, or by coating the tendon with a resin of known, low, shear strength. Both of these types of partial bonding are described below.

Intermittent bond

In this system, discrete *lengths* of FRP tendon are alternately bonded and debonded (see Figure 3). By intermittently debonding the tendon, the length over which the tendon can strain is controlled.

Figure 3a shows part of a concrete beam, subject to a sagging bending moment. A pre-tensioning tendon which is alternately bonded (B) and unbonded (UB) to the concrete passes through this region. In general, the unbonded lengths will be longer than the bonded lengths.

In the figure, the bonded sections are denoted by open boxes and are prefixed with ‘B’ whereas the unbonded sections are represented as a thin line and are prefixed with ‘UB’. A subscript is used to identify a particular tendon segment. The tendon forces, T , along the length of the tendon are also shown.

Before loading, the tendon forces in all the regions are equal to the initial prestress

force, P_0 . When a load is applied, the compressive strain in the concrete decreases on the lower face until a crack forms. For the purposes of illustration, it will be supposed that this crack intersects segment UB3; the force in this segment will increase to the level T_3 .

The subsequent behaviour depends on the length of the adjacent bonded segments. If the bonded lengths are *insufficient* to carry the difference between the ultimate capacity of the tendon and the initial prestress force, the bond will break down during loading (Figure 3b). Hence, the extent and distribution of the bonded sections can be designed so that when the force in a particular unbonded segment, say UB3, approaches a pre-determined threshold, the bond in an adjacent bonded segment (say, B2) will break down and force would be transferred to UB1. This type of controlled bond failure prevents any individual segment from becoming over-stressed and causing a brittle failure, at least until the neighbouring regions are fully stressed.

An alternative case arises if the bonded lengths are *sufficient* to transfer the difference between the ultimate capacity of the tendon and the initial prestress force; the bond will not then break down during loading (Figure 3c). Hence, in this scenario, even when the force in segment UB3 approaches the breaking load of the tendon, there is no transfer of force from UB3 to UB1 or from UB3 to UB5. The rotation at the crack location will be dependent only on the length of the unbonded region, UB3.

Coating of tendon

Another possibility is to reduce the bond strength between the tendon and the concrete by coating the tendon with a resin adhesive. The properties of the resin

should be such that only small bond stresses can be sustained, which controls the rate at which force can build up in the tendon along its length. As a result, when cracking occurs, the force in the tendon varies over a significant length on either side of the crack. The length required to transmit the additional force to the tendon is a function of the resin shear strength and is related to the angle β (as shown in Figure 4). The angle β reflects the change in force with length, and the distribution of tendon force due to three different values of β are shown in the figure (a constant bond stress distribution has been assumed). In each case the force T_3 and the length L_{ab} vary, and the analysis is complex; the force T_3 must satisfy overall equilibrium of the section, and the triangle of length L_{ab} and height $T_3 - P_o$ is related to the additional extension of the tendon, which must satisfy overall compatibility conditions. This analysis will be described elsewhere.²

After transfer, the force in the tendon at locations 1, 3 and 5 are all equal to the initial prestress force, P_o . If a crack occurs at 3 there will be an increase in the tendon force at this location. The rate at which this force increase can be transmitted along the tendon is governed by the value of β , which will thus dictate the tendon length which is affected by the force increase.

The magnitude of β has an important influence on the behaviour of the beam. If β is too large then the strain near the crack occurs over only a small length of tendon and although the increase in force is quite high, the extension of the tendon will be minimal. As a result only small rotations will occur and the behaviour of the beam will be similar to that of beams with fully-bonded tendons (Figure 4c). If the value of β is too small then, after first cracking, the tendon strains over such a long length

that the flexural response becomes analogous to beams with unbonded tendons. So, although large rotations are realised, the moment capacity would be expected to be reduced (Figure 4d).

Hence, a judicious choice of β is required which is low enough to ensure large rotations but large enough to ensure that adequate forces develop at the crack interface. In this way, a distributed crack pattern will result and the tendon will be able to achieve its full capacity prior to concrete crushing.

TEST PROGRAMME

The main experimental programme was designed to demonstrate the influence of the bond between an AFRP tendon and concrete on the flexural response of a pre-tensioned concrete beam. Beams with fully-bonded, unbonded and partially-bonded tendons were considered.

Design philosophy

Concrete beams pre-tensioned with small diameter AFRP tendons were cast and tested. Two types of AFRP tendon, a braided rod comprised of Kevlar 49 fibres in an epoxy resin (FiBRA) and a spiral wound pultrusion with Technora fibre in a vinylester matrix (Technora rod), were used (see Figure 5). Beams with steel tendons were included in the bonded and unbonded test series for comparison purposes. The properties of the three tendon materials can be found in Table 1.

The use of small diameter tendons was deemed to be advantageous since specimen sizes could be kept to a minimum and a pre-tensioned system was chosen since it avoided the need for long-term anchorages. However, the provision of even a temporary

anchoring system proved to be problematic. A stressing system based on the use of expansive cement couplers was eventually chosen.¹⁰

It was proposed that the strands be tensioned to approximately 70% of their ultimate strength. A high proportion of the creep and relaxation experienced by the FRP tendons occurs soon after tensioning. It was therefore expected that by the time the beams were tested the tendons would be stressed to approximately 60-65% of their ultimate capacity. This seemed to be a practical level of prestressing and, in view of the time-scale of the experiments, long-term stress rupture would not be an issue at these levels of prestressing.¹¹

In order to have similar ultimate load capacities for both the AFRP beams, the beams with the braided AFRP contained 3 no. 3.7 mm diameter tendons whereas the beams with the spiral wound AFRP contained 2 no. 4 mm diameter tendons. The beams with prestressing steel were stressed using 2 no. 5 mm diameter tendons which were part of the laboratory's stock. In each case the centroid of the tendons was located in the middle third of the beam (see Figure 6). The section sizes ($100 \times 200 \times 2800$ mm) and prestress levels were the same in all cases but the extent and distribution of the bond between the concrete and the tendon varied. All the beams were tested in flexure using a four point loading arrangement (see Figure 6). For the partially-bonded beams, an 8 mm high triangular crack inducer was included at the centre of the beam thereby reducing the beam depth at this section. This was primarily intended to fix the location of the first crack so that the beam could be properly instrumented.

The test series included beams with fully-bonded, unbonded, intermittently-bonded and adhesive-bonded tendons. In all cases, the ends of the tendon remained bonded to

the concrete to ensure the integrity of the tendon anchorage.

Fully-bonded and unbonded beams

The fully-bonded beams were designed to fail due to tendon rupture. In contrast, the unbonded beams, where the central portion of the tendon was debonded from the concrete, were expected to fail as a result of concrete crushing.

Intermittently-bonded beams

The first series of intermittently-bonded beams were designed so that, as the force on one side of the bonded section reached a certain threshold, the bond would break down and the force would be transmitted to an adjacent length of tendon. This would be designed to occur before the more highly stressed element ruptured.

Based on the results of a series of prestressed pull-out tests¹², it was clear that a significant bond stress could be transmitted through very short bonded lengths of tendon. A bond length of 15 mm was chosen to encourage the bond to break down when the tendon reached a force of approximately $0.80 P_{ult}$, where P_{ult} is the breaking load of the tendon. To investigate possible effects due to an asymmetrical distribution of bond, the lengths of the bonded tendon segments on one side of the beam were increased to 20 mm (see Figure 7c).

In the second series of intermittently-bonded beams, the bonded lengths were much longer (100 mm) and more indicative of a length that would be considered in the design of a prototype beam (see Figure 7d). However, as a result, the bond was unlikely to break down during testing and the tendon would snap, although at a larger rotation than for the fully-bonded beams.

Adhesive-bonded beams

The goal of the adhesive-bonded tests was to determine the effect of limiting the bond between the tendon and the concrete by coating the tendon with a resin (see Figure 7e). Tests were carried out to give an initial insight into the bond strength of the adhesive.¹²

Experimental procedure

The use of a Rapid Hardening Portland Cement mix to obtain a high strength at an early age optimised the casting/testing programme (a compressive cube strength of approximately 60 MPa was achieved after 7 days). Because of the low water cement ratio (0.37), a superplasticiser was added to the mix to improve workability.

The casting rig was designed so that two beams could be cast at the same time (see Figure 8). The de-tensioning system was such that the prestress force would be released gradually.

The test set-up was incorporated in a stiff reaction frame. The loads were applied using two 10 tonne (100 kN) hydraulic jacks, each with 100 mm extension (see Figure 9).

Experimental methodology

The AFRP tendons were prepared to suit the particular test series. The fully-bonded tendons required no treatment. For the unbonded and partially-bonded tendons, the unbonded regions were formed by covering the tendons in appropriate lengths of plastic tube.

The manufacture of the adhesive-bonded tendons was complex and several trials were required to optimise the procedure of applying the adhesive to the tendons. Visual

and tactile observations of the coated tendons indicated that the coating of the braided AFRP resulted in a smooth outer surface. The coating of the spiral wound AFRP was not sufficiently thick to fully coat the outer spiral winding, so small deformations were still present on the outer coated surface. The average coated tendon diameter for the braided and spiral wound AFRPs were 4.0 mm and 4.5 mm respectively.

After the necessary tendon preparations had been completed, both ends of the AFRP tendon were connected to pieces of prestress wire using the expansive cement couplers described elsewhere.¹⁰ A schematic representation of this system can be found in Figure 10. The steel/AFRP/steel tendon was stressed and anchored using standard equipment for the stressing of steel wire.

In order to monitor the load in the tendons during tensioning, two 5 mm strain gauges were attached to each piece of the steel prestress wire. The gauges were attached in parallel on either side of the tendon to mitigate the effects of any flexural strains in the steel. Strain gauges were not attached to the AFRP for the following reasons:

- Conventional strain gauges have a maximum range of 2% elongation. The elongation capacities of the FiBRA and Technora are 2% and 3.7% respectively.
- The strain gauges would measure the strain in the resin which would not necessarily be representative of the strain in the FRP composite.
- The surface profiles of the AFRPs were not conducive to the attachment of gauges; the diameter of the FiBRA was only 3.7mm and the rod was braided; the diameter of the Technora was 4mm and the rod was characterised by closely spaced spiral wrappings.

However, the repercussion of this decision is that the tendon forces and bond stresses during testing could only be determined through a back analysis of the experimental results. Details of this analysis will be the subject of a companion paper.²

The tendons were tensioned individually using a hand-powered PSC single wire jack with a capacity of about 70 kN. The rate of tensioning was approximately 1 kN per minute. The load in the tendon was monitored using the strain gauges attached to the steel prestress wire. To confirm the force in the tendon the load in the jack was also monitored and the overall extension of the tendon noted. After the required stress level was reached, the live end of the tendon was locked off and the procedure was repeated until all the tendons had been tensioned. Almost immediately after tensioning, the concrete beams were cast around the free length of aramid tendon located between the couplers. By this time, the stress level in the tendons had dropped to about 65% of the manufacturer's assured load, primarily as a result of a large short-term relaxation associated with the AFRP materials.

The concrete was batched in the laboratory using a pan mixer and two batches were required for each set of beams. Three concrete cubes (100×100 mm), two concrete cylinders (100×200 mm) and two modulus of rupture specimens (100×100×500 mm) were cast from each batch.

After casting, the beams were covered with polythene sheet and left in the mould for a period of three days. The formwork was then removed and the necessary gauges attached. The beams were typically de-tensioned five days after casting and the average concrete cube strength was found to be 55 MPa at transfer. Prior to transfer, the prestress levels in the tendons were, in general, around 63-65% of the manufacturers'

assured loads.

Testing of Beams

In most cases, testing was carried out seven days after casting. Portal gauges were attached along the length of the beam in order to measure the strains at set positions. LVDT's were used to monitor the displacements of the beam. Strain hoops to measure slip were connected at either end of the tendons and load cells were placed under the jacks (see Figure 11). The electronic gauging equipment was monitored using a data logger and the time at which a reading was taken was manually controlled. In addition, the crack patterns were visually noted and the patterns monitored throughout testing. The beams were loaded monotonically until failure.

The control specimens were tested on the same day as the beams. In several cases displacement-control tests were carried out on the concrete cylinders to ascertain the concrete stress-strain relationships. The value of the modulus of elasticity for the specimens varied between 21,000 MPa and 22,500 MPa. The average modulus of elasticity, E_c , was 22,000 MPa and the average strain at the ultimate load, ϵ_{cu} , was approximately 0.0030.

As it was not possible to measure directly the prestress in the AFRP tendons, the force in the coupled steel prestress wire at the time of de-tensioning (day 5) had to be extrapolated to estimate the force in the AFRP tendons at the time of testing (day 7). Preliminary calculations suggested that the total losses due to concrete creep, concrete shrinkage and tendon relaxation were small (1.6% for FiBRA, 1.2% for Technora). Hence, the prestress force at the time of de-tensioning was taken to be representative

of the level of prestress at the time of testing without introducing a significant loss of accuracy.

EXPERIMENTAL RESULTS

During the testing of the beams, both the cracking and the load-deflection behaviour were monitored.

Crack patterns and behaviour

In the AFRP beams, as a crack formed it grew almost instantaneously to a height of approximately 140 mm above the base of the beam. The crack growth in the steel beams was much less dramatic and immediately after a crack occurred, the crack height was between 40 mm and 60 mm above the base of the beam. The rapid crack growth occurred in all the AFRP beams and was attributed to the low modulus of elasticity of the aramid tendons. The crack patterns for each beam series were quite distinct.

The cracks in the fully-bonded series were fairly uniformly distributed. Fork-like patterns were noted in the cracks in the constant moment region whereas the cracks that occurred in the shear span tended not to fork but to propagate towards the load points (see Figure 12a-c).

The unbonded series was notable in that usually only a single crack occurred in each beam (see Figure 12d-f). In the beams with either steel or spiral wound AFRP tendons, the crack occurred close to the centreline of the beam. In the beam with braided AFRP tendons, the crack was offset 300 mm from the beam centreline. After the occurrence of the first crack, extensive horizontal cracking was noted with increasing load.

In both the first intermittently-bonded series (where the bond was expected to break

down during testing) and the second intermittently-bonded series (where the bond was not expected to break down during testing), three cracks occurred in the AFRP beams (see Figure 13a-d).

Qualitatively, the greatest differences between the two types of AFRP beam behaviours were noted in the adhesive-bonded beams (see Figure 13e-f). In the spiral wound AFRP beam, the central crack occurred at the crack inducer and, as the load increased, a second crack formed. However, no further cracks occurred and it was found that the second crack closed upon subsequent loading. A minimal amount of rotation took place at the second crack and the behaviour as the beam approached failure was similar to that of the unbonded beams. In contrast, the braided AFRP beam cracked in three places with large rotations occurring at each crack location. All three cracks occurred in the constant moment region.

Ultimate loads

The ultimate loads and failure modes for the experimental beams can be found in Table 2. The load P_u represents the applied load, in excess of the beam dead-weight, which resulted in the failure of the beam. The concrete compressive cube strength and the concrete tensile strength are denoted by f_{cu} and f_t respectively.

It should be noted that the fully-bonded AFRP beams failed due to tendon rupture. In contrast, the unbonded AFRP beams failed at a lower load due to concrete crushing. Half of the partially-bonded beams failed due to concrete crushing (TIB1, FIB1, and TAB).

There was one partially-bonded case where failure was due to the tendons rupturing

(FIB2) and two cases where concrete crushing and tendon rupture appeared to occur simultaneously (TIB2, FAB). The failure of both the concrete and the tendon at the same time would represent the most efficient use of the composite.

Load-deflection curves

The load-deflection curves for the AFRP beams can be found in Figure 14. A drop-off in load was noted after the occurrence of each crack.

DISCUSSION OF BEAM BEHAVIOUR

During the testing of the *fully-bonded* beams, a noticeable curvature was observed through the constant moment region. Numerous cracks occurred but the rotation at each crack location was limited. The ultimate capacity of these beams was high as failure was due to tendon rupture. However, only a small amount of deflection had taken place prior to the brittle failure.

In the *unbonded* beams, large deflections were exhibited (approximately twice those of the fully-bonded beams). The crack in the constant moment region acted as a hinge and the sections of beam on either side of the crack behaved as rigid bodies. However, high localised strains were generated in the concrete at the hinge location and final failure was due to the premature concrete crushing at the hinge. The ultimate load capacity was 25% lower than that of the fully-bonded beams.

In all cases, the deflections of the *partially-bonded* beams were greater than those of the fully-bonded beams and, with the exception of the adhesive-bonded beam with spiral wound AFRP tendons, the partially-bonded beams had higher ultimate load capacities than the unbonded beams. As in the unbonded beams, the flexural cracks seemed to

act as hinge locations and the sections of beams connected by the hinges appeared to behave as rigid blocks. The formation of multiple cracks was a crucial element in ensuring the enhancement of the rotation capacity of these beams. Furthermore, the development of cracks was intrinsically connected to the extent and distribution of the bond along the tendon. After first cracking, the occurrence of the second crack was a function of the magnitude of force that the tendon could transmit to the concrete through the bonded sections. If this force was less than a critical value, then second cracking did not occur. An overview of aspects of the interaction between the cracking behaviour and the tendon force are detailed elsewhere.¹³

One potential drawback to a smaller number of cracks in the partially bonded beam (when compared with the fully-bonded beams) is that there will possibly be less evidence of pending failure. However, after the formation of a crack the subsequent rotations of the partially-bonded beams were higher than those of the fully-bonded beams. Hence, the presence of fewer visible cracks would be compensated by larger deflections. A key feature of the partially-bonded system is that the large rotations are a characteristic of the ultimate limit state design. Under service loading the beam would be expected to remain uncracked.

As discussed earlier, the current work focused on the rotation capacity of the beams and did not directly address the question of ductility. In order to quantify the portion of inelastic energy in the system, it would be necessary to unload the beams just prior to failure and to measure the extent of the inelastic deformation. From the inelastic deformation, one could then postulate both the total and elastic energy in the system. Unfortunately, as it is often difficult to predict the failure load, finding the exact point

at which to unload is problematic and hence load-cycling is required. In addition, Vijay et al.¹⁴ found that, in beams which failed by concrete crushing, the inelastic energy was highly dependent on the stage at which the load was released at the onset of the compressive failure.

In partially-bonded beams it is expected that the total energy input into the system will result in a combination of the following actions; the extension of the tendon, the straining of the concrete in compression, possible dowel action, the formation of cracks in the concrete, aggregate interlock, the debonding of the tendon from the concrete and the frictional bond resistance. As the beams were tested monotonically until failure it is not possible to make definitive statements about the relative amounts of elastic and inelastic energy (the residual inelastic deformations were not measured). However, it is important to note that the tendon extension is linearly elastic (except for possibly a small amount of creep) and it is expected that this will be a dominant component of the total energy of the system. Some inelastic energy will be dissipated in the concrete hence the beams which exhibited large rotations are likely to have a higher plastic energy absorption than the beams with small rotation capacities. The possibility of enhancing this energy absorption is the subject of current research.

From the experimental results, it can be seen that the concept of partial bond has far-reaching implications for the flexural design of concrete pre-tensioned with FRP tendons (a discussion of these implications can be found elsewhere¹⁵). By controlling the bond at particular locations along the beam, the designer can optimise both the ultimate capacity and the rotation capacity of a beam.

Although the principle of partial bond is promising, further work is necessary to en-

sure the long-term performance of the system. Additional areas requiring investigation would include: the fatigue behaviour of the intermittently and adhesive-bonded beams; the long term integrity of the bond and the effect of the intermittent or the adhesive bond on the shear capacity of the beam.

CONCLUSIONS

The energy considerations in an FRP-prestressed beam are very different from those of a similar beam with steel tendons. There is little ductility in FRP systems and thus the rotation capacity of these systems is of great importance. Failure due to tendon rupture is brittle and sudden.

In the main experimental series, small-scale ($100 \times 200 \times 2800$ mm) fully-bonded, unbonded and partially-bonded pre-tensioned concrete beams were cast. The beams were tested under four-point loading until failure. The fully-bonded beams had a high ultimate load capacity and failed due to tendon rupture. However, only limited rotations occurred prior to failure. During the testing of the unbonded beams a single crack formed and, although large rotations were apparent, premature failure occurred due to concrete crushing. The ultimate load capacity of the unbonded beams was significantly lower (25%) than that of the fully-bonded beams.

The partially-bonded beam tests were extremely successful and, with the exception of the adhesive-bonded beam with spiral wound AFRP tendons, all the partially-bonded beams had a high ultimate load capacity and a large rotation capacity. The beams appeared to act as a series of rigid blocks connected by hinges, and the formation of multiple cracks was a crucial element in ensuring that premature concrete crushing did

not occur (as evidenced in the unbonded beams). In two of the beams, the adhesive-bonded braided AFRP beam and the second intermittently-bonded spiral wound AFRP beam, an ultimate load capacity equivalent to that of the fully-bonded beams was achieved. It was demonstrated that the idea of partial bonding could be used to optimise the flexural response of concrete beams pre-tensioned with FRP tendons.

ACKNOWLEDGEMENTS

The authors are grateful for the support of Chichibu Onoda Cement Co., Teijin Ltd, Mitsui Construction Co. and Tarmac Precast Concrete Ltd. Kevlar is a trade name of Du Pont, Technora of Teijin and FiBRA of Mitsui. One of the authors (JML) was sponsored by the Natural Sciences and Engineering Research Council of Canada (NSERC) and is appreciative of NSERC's financial assistance.

NOTATION

B	bonded segment
E_c	modulus of elasticity of concrete
E_t	modulus of elasticity of tendon
f_{cu}	concrete compressive cube strength
f_t	modulus of rupture tensile strength of concrete
L_{ab}	bond breakdown length of adhesive bonded tendon
L_b	bonded length of tendon segment
L_{ub}	unbonded length of tendon segment
P_o	initial prestress force
P_u	ultimate applied load

P_{ult}	manufacturer's assured load for tendon
T	force in tendon segment
UB	unbonded segment
V_f	volume fraction of fibres
β	angle relating to the change in force with length
ϵ_{cu}	ultimate concrete compressive strain at failure
ϕ	bar diameter

References

- [1] C. J. Burgoyne. Should FRP be bonded to concrete? In A. Nanni and C. W. Dolan, editors, *Fiber-Reinforced-Plastic Reinforcement for Concrete Structures - International Symposium, SP-138*, American Concrete Institute, March 1993, pp. 367-380.
- [2] J. M. Lees and C. J. Burgoyne. Analytical study of the influence of bond on the flexural behaviour of concrete beams pre-tensioned with AFRPs, *in preparation*.
- [3] A. Nanni, T. Okamoto, M. Tanigaki, and S. Osakada. Tensile properties of braided FRP rods for concrete reinforcement. *Cement & Concrete Composites*, 15(3), 1993, pp. 121-129.
- [4] K. Noritake, R. Kakihara, S. Kumagai, and J. Mizutani. Technora, an aramid FRP rod. In A. Nanni, editor, *Fiber-Reinforced-Plastic (FRP) Reinforcement for Con-*

- crete Structures: Properties and Applications*, Developments in Civil Engineering, 42, Elsevier Science Publishers B.V., 1993, pp. 267-290.
- [5] H. Mera and T. Takata. High performance fibers, *Ullmann's Encyclopedia of Industrial Chemistry*, volume A 13. VCH, 5th edition, 1989.
- [6] Teijin Ltd. *High Tenacity Aramid Fibre - Technora*. Technical Information - TIE-05/89.11, 1989.
- [7] T. Tamura. FiBRA. In A. Nanni, editor, *Fiber-Reinforced-Plastic (FRP) Reinforcement for Concrete Structures: Properties and Applications*, Developments in Civil Engineering, 42, Elsevier Science Publishers B.V., 1993, pp. 291-303.
- [8] M. Tanigaki, T. Okamoto, T. Tamura, S. Matsubara, and S. Nomura. Study of braided aramid fiber rods for reinforcing concrete. *IABSE, 13th Conference, Helsinki*, 1988, pp. 15-20.
- [9] R. Kakihara, M. Kamiyoshi, S. Kumagai, and K. Noritake. A new aramid rod for the reinforcement of prestressed concrete structures. In *Advanced Composites Materials in Civil Engineering Structures Proceedings, Las Vegas, Jan. 31, 1991*, MT Div/ASCE, Jan. 31 1991, pp. 132-142.
- [10] J. M. Lees, B. Gruffydd-Jones, and C. J. Burgoyne. Expansive cement couplers - A means of pre-tensioning fibre-reinforced plastic tendons. *Construction and Building Materials*, 9(6), 1995, pp. 413-423.
- [11] A. Gerritse. Specific features and properties of AFRP-bars. In M. M. El-Badry, editor, *Advanced Composite Materials in Bridges and Structures - 2nd Interna-*

tional Conference, The Canadian Society for Civil Engineering, Montreal, Quebec, Canada, 11-14 August 1996, pp. 75-82.

- [12] J. M. Lees. *Flexure of Concrete Beams Pre-tensioned with Aramid FRPs*. PhD thesis, Department of Engineering, University of Cambridge, UK, 1997.
- [13] J. M. Lees and C. J. Burgoyne. Rigid body analysis of concrete beams pre-tensioned with partially bonded AFRP tendons. In *Non-Metallic (FRP) Reinforcement for Concrete Structures, Proceedings of the Third International Symposium, Sapporo, Japan*, Volume 2, Japan Concrete Institute, October 1997, pp. 759-766.
- [14] P. V. Vijay, S. V. Kumar, and H. V. S. GangaRao. Shear and ductility behavior of concrete beams reinforced with GFRP rebars. In M. M. El-Badry, editor, *Advanced Composite Materials in Bridges and Structures - 2nd International Conference*, The Canadian Society for Civil Engineering, Montreal, Quebec, Canada, 11-14 August 1996, pp. 217-226.
- [15] C. J. Burgoyne. Rational use of advanced composites in concrete. In *Non-Metallic (FRP) Reinforcement for Concrete Structures, Proceedings of the Third International Symposium, Sapporo, Japan*, Volume 1, Japan Concrete Institute, October 1997, pp. 75-88.

Biographical Sketches

Janet Lees completed her Ph.D. studies at the University of Cambridge, UK in 1997 and is currently working as a post-doctoral researcher at the Swiss Federal Laboratories for Materials Testing and Research. Her research interests include the use of fibre reinforced plastics in construction applications and the behaviour of concrete structures.

Chris Burgoyne is a lecturer at the University of Cambridge, UK. He has been working with advanced composites applied to concrete structures since 1982. He is a member of ACI 440, and convenor of the Institution of Structural Engineers Study Group on Advanced Composites.

Table 1 : Tendon and fibre material properties^{5,6,7,8,9}

Table 2 : Experimental results - Ultimate loads

Table 1 : Tendon and fibre material properties^{5,6,7,8,9}

Material	Density (kg/m ³)	Fibre Type	Young's Modulus (GPa)	Max. Elong. (%)	Tensile Stren. (MPa)	V _f (%)
braided FiBRA	1.28	Kevlar 49	68.6	2.0	1480	65-70
Kevlar 49 fibre	1.45	Kevlar 49	120.0	2.5	2800	100
spiral wound Technora	1.3	Technora	54.0	3.7	1900	65
Technora fibre	1.39	Technora	73.0	4.6	3400	100
Steel (high yield)	7.8	n/a	200	10.0	650	n/a
Steel (prestress)	7.8	n/a	220	4.2*	1760	n/a

* measured value

Table 2 : Experimental results - Ultimate loads

Beam	Prestress (kN)	f_{cu} (MPa)	f_t (MPa)	P_u (kN)	Fail Mode
SB (1)	42.5	67.8	3.1	10.4	conc
SB (2)	44.4	70.9	3.1	10.1	conc
TB (1)	30.7	58.5	3.0	8.0	tendon
TB (2)	31	58.5	3.0	8.0	tendon
FB	28	68.5	3.2	7.8	tendon
SUB (1)	49.9	60.8	3.9	9.8	conc
SUB (2)	46.3	65.6	3.7	9.6	conc
TUB	28.4	60.3	3.3	6.2	conc
FUB	29.8	60.3	3.3	6.3	conc
TIB1	29.3	56	3.4	7.0	conc
TIB2	29.3	56.3	3.1	7.8	tendon/conc
FIB1	29.1	56	3.4	7.4	conc
FIB2	30.5	56.3	3.1	7.4	tendon
TAB	29.1	58	3.2	6.4	conc
FAB	30.1	58	3.2	7.9	tendon/conc

Each beam is identified by a series of letters and, in some cases, a number. The first letter indicates the type of tendon material, the next set of characters identifies the tendon bond condition and a number in brackets is used to distinguish between several beams of the same type. The key is as follows:

S: 5 mm steel prestress wire B: fully-bonded tendon: tendon breaking
T: 4 mm spiral wound AFRP rod UB: unbonded conc: concrete crushing
F: 3.7 mm braided AFRP rod IB1/2: intermittently-bonded series 1/2
AB: adhesive-bonded

Figure 1 : Schematic stress-strain curves for different types of FRPs (within each category of FRP, the materials will vary both in terms of strength and modulus of elasticity)

Figure 2 : Schematic load-deflection curves

Figure 3 : Intermittently-bonded tendons

Figure 4 : Tendon coated with adhesive

Figure 5 : AFRP rods *after Nanni et al.*³, *Noritake et al.*⁴

Figure 6 : Beam cross sections and loading arrangement

Figure 7 : Tendon details

Figure 8 : Photograph of casting rig

Figure 9 : Photograph of testing rig

Figure 10 : Diagram of stressing system using expansive cement couplers (schematic)

Figure 11 : Experimental gauges for beam tests (schematic)

Figure 12 : Crack patterns - Fully-bonded and unbonded beams (schematic)

Figure 13 : Crack patterns - Partially-bonded beams (schematic)

Figure 14 : Load-deflection curves for AFRP beams

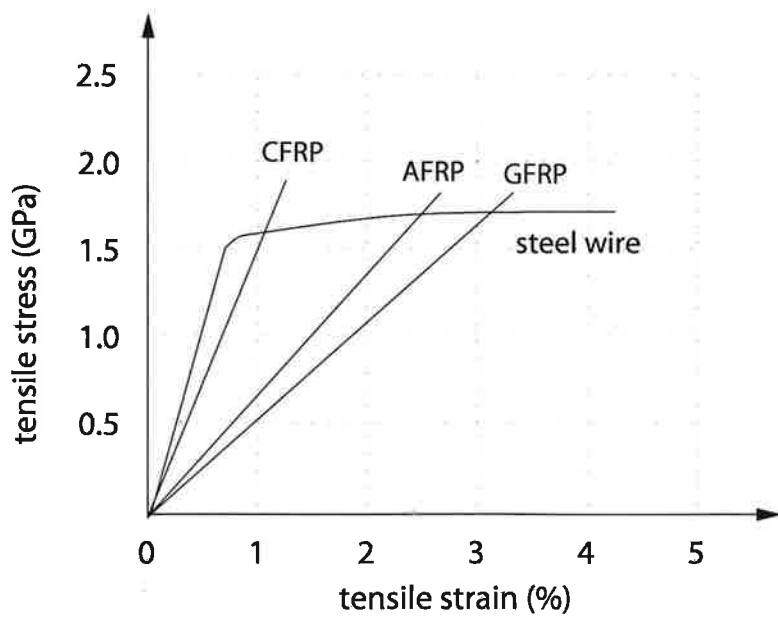


Figure 1 : Schematic stress-strain curves for different types of FRPs (within each category of FRP, the materials will vary both in terms of strength and modulus of elasticity)

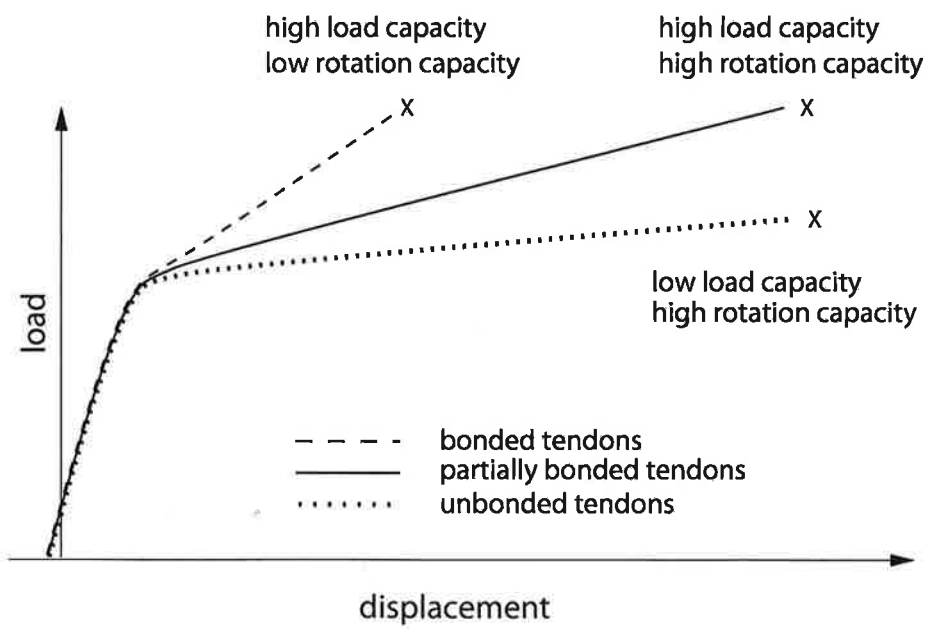
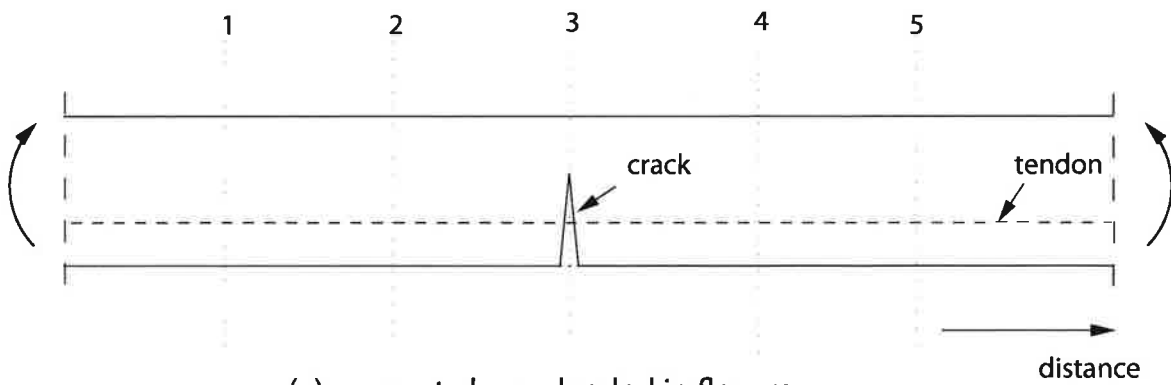
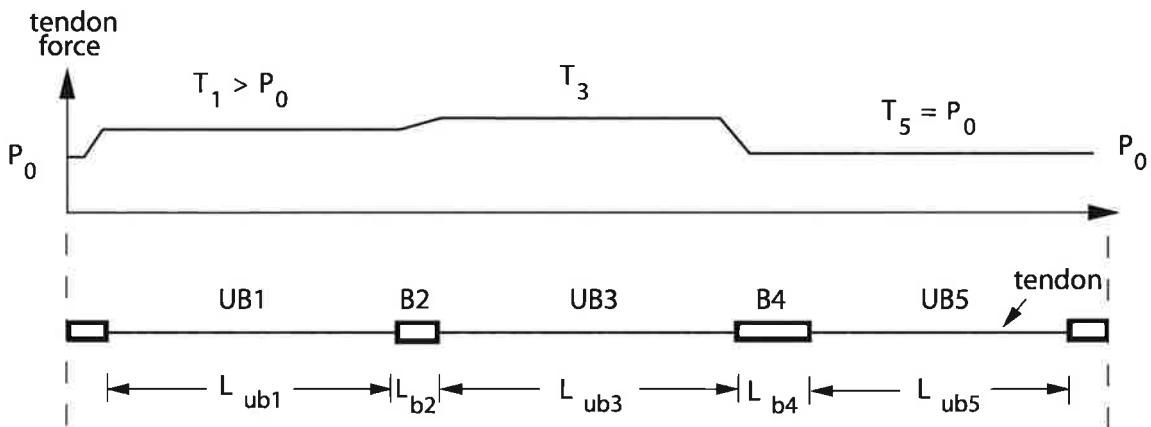


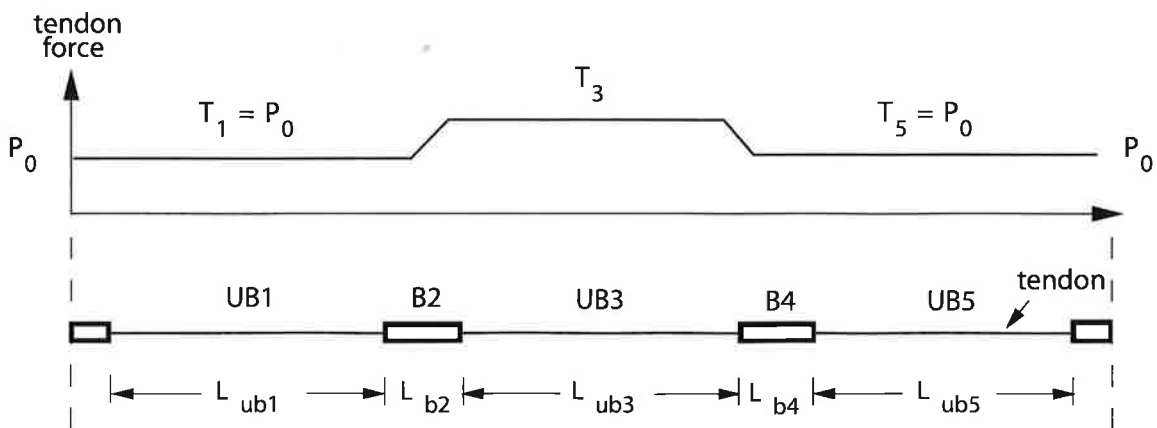
Figure 2 : Schematic load-deflection curves



(a) concrete beam loaded in flexure



(b) bond breaks down in segment B2



(c) bond does NOT break down

bonded segment
 unbonded segment

Figure 3 : Intermittently-bonded tendons

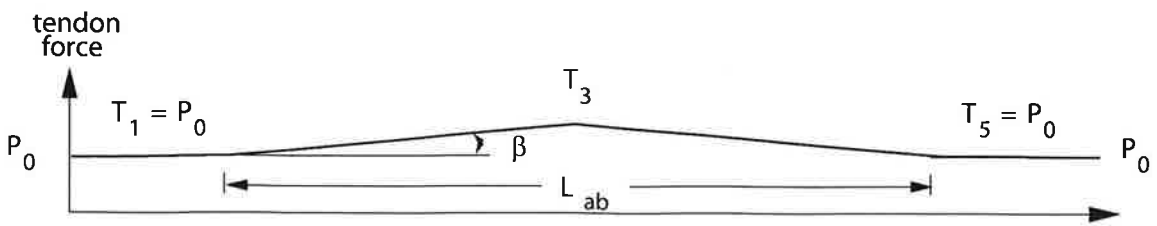
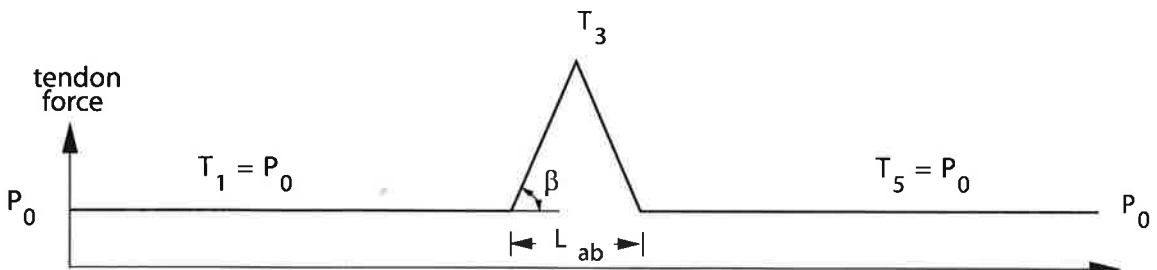
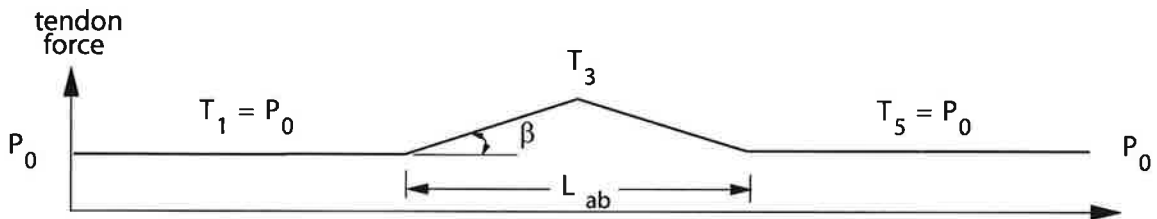
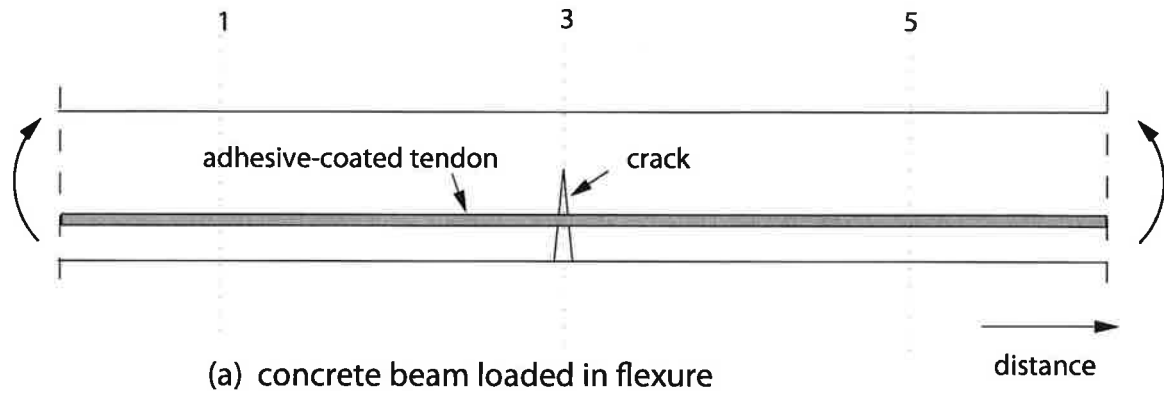


Figure 4 : Tendon coated with adhesive

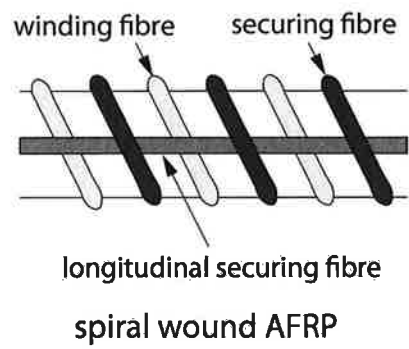
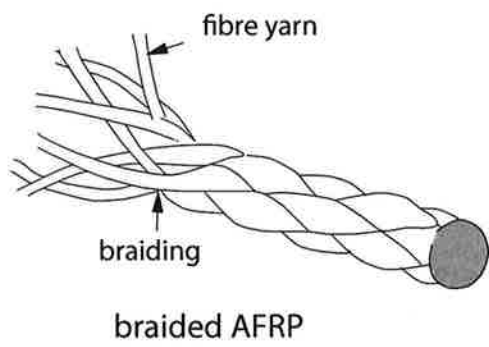
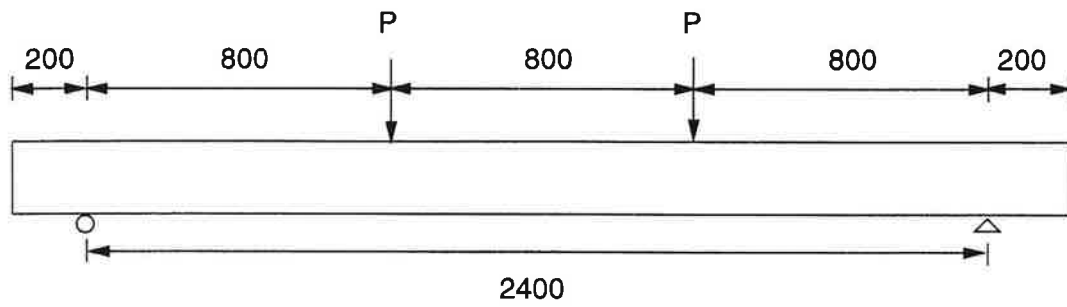
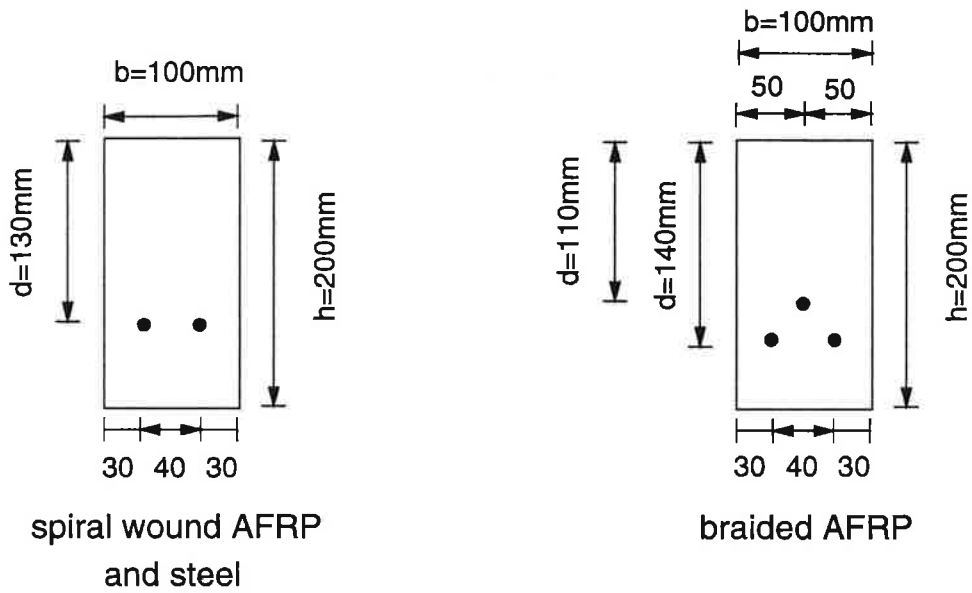


Figure 5 : AFRP rods after Nanni et al.³, Noritake et al.⁴



Note: all dimensions in mms

Material	No. of tendons	E_t (MPa)	Parameters for a single tendon		
			ϕ (mm)	area (mm ²)	P_{ult} (kN)
braided AFRP	3	68,600	3.7	11	15.7
spiral wound AFRP	2	54,000	4	12.6	22.7
steel	2	220,000	5	19.6	34.4

Figure 6 : Beam cross sections and loading arrangement

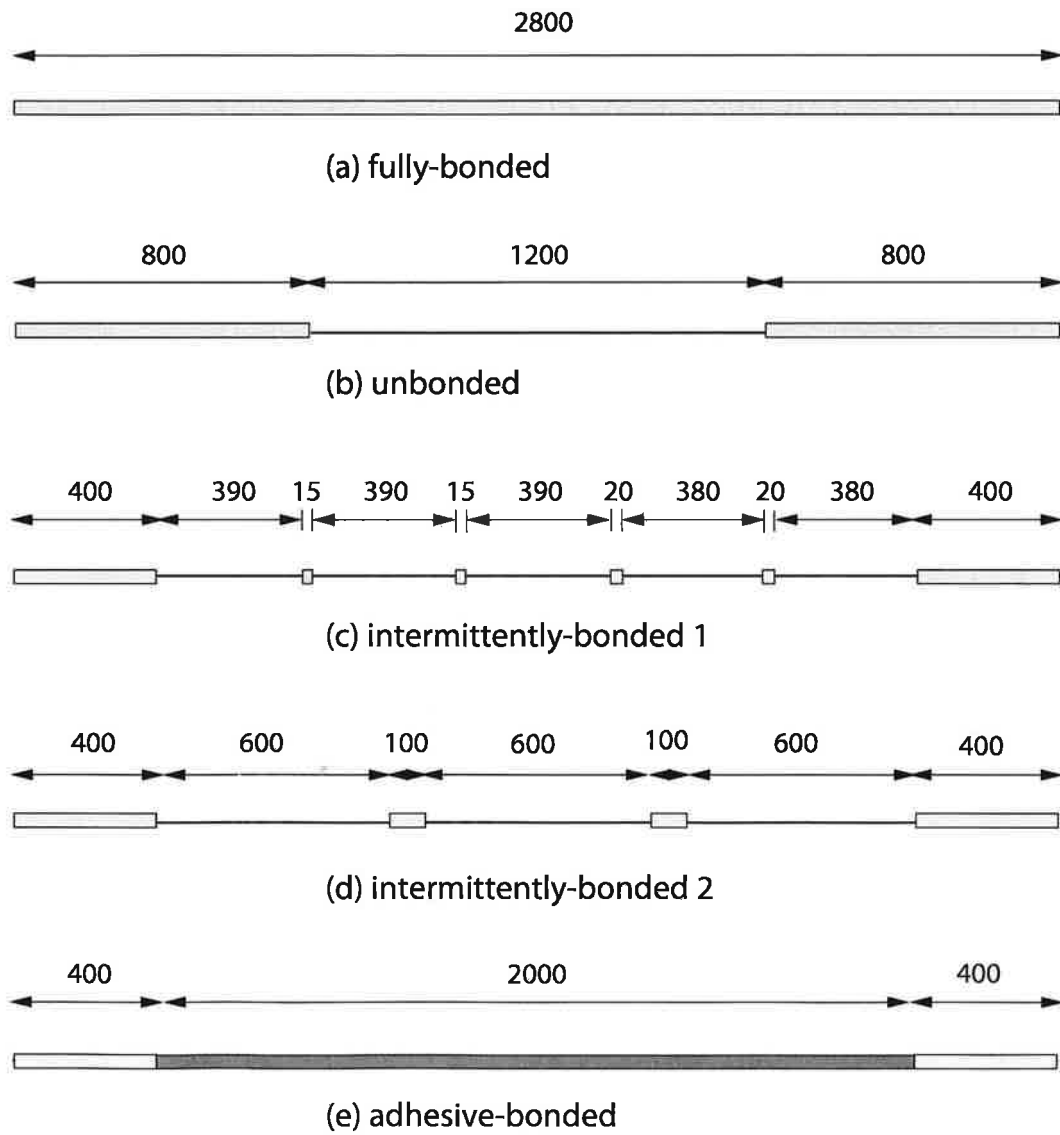


Figure 7 : Tendon details

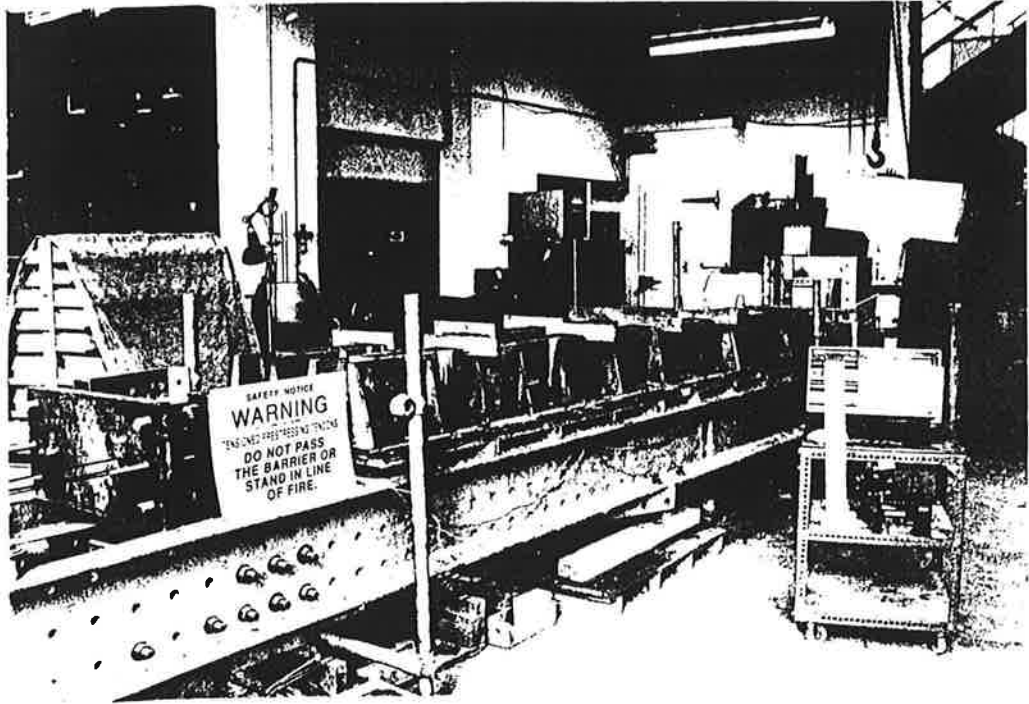


Figure 8: Photograph of casting rig

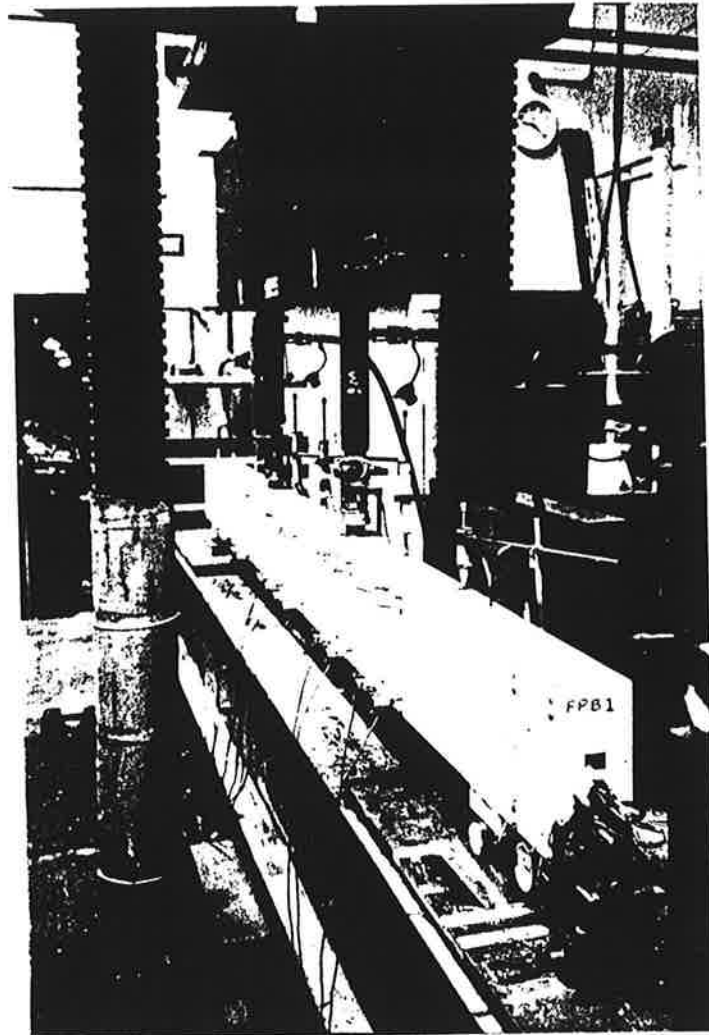


Figure 9: Photograph of testing rig

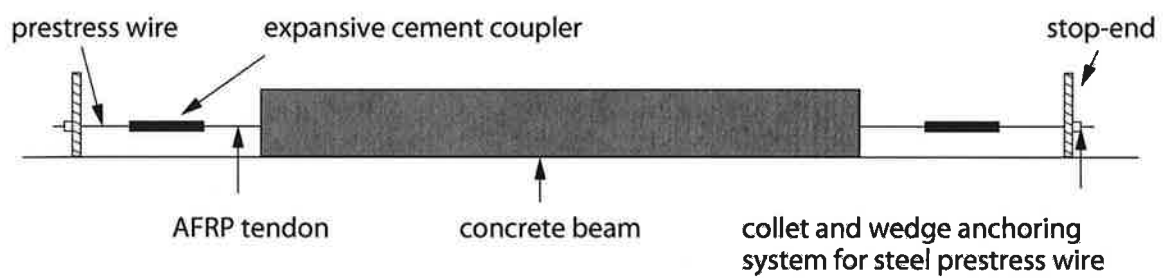


Figure 10 : Diagram of stressing system using expansive cement couplers (schematic)

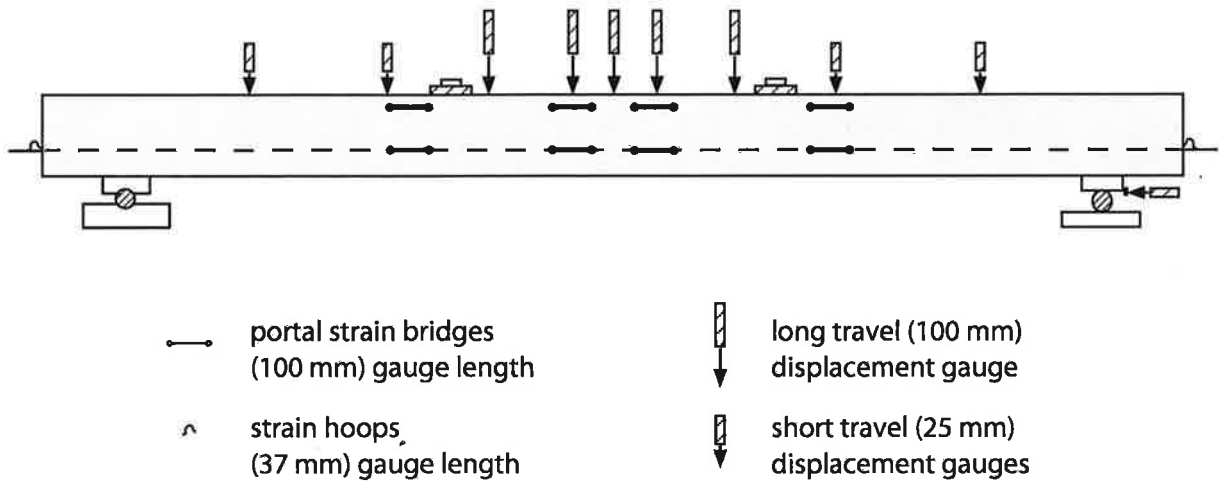
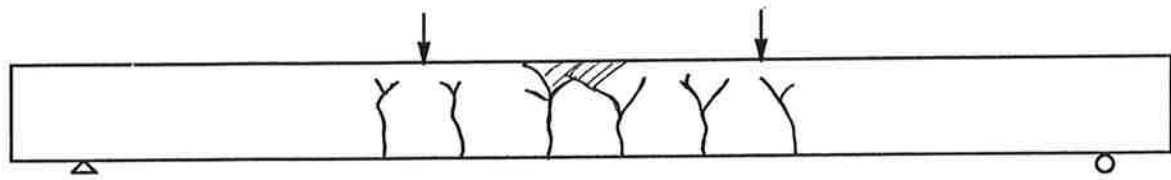
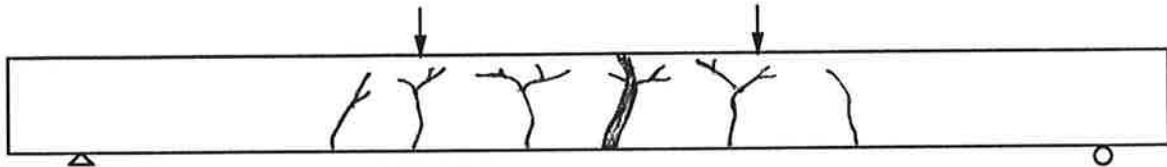


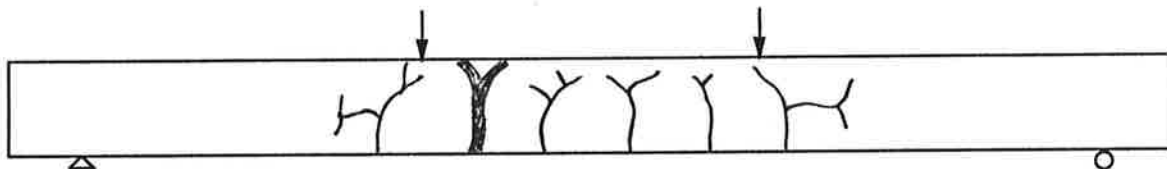
Figure 11 : Experimental gauges for beam tests (schematic)



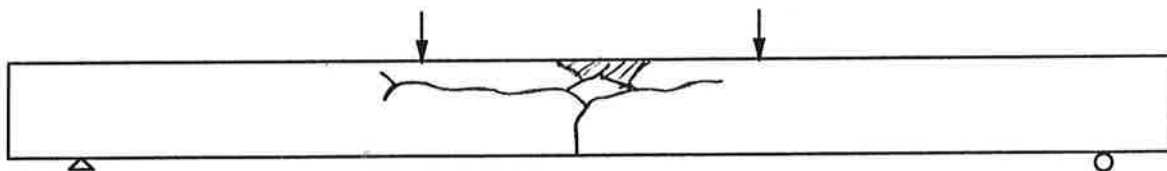
(a) fully-bonded beam with steel tendons



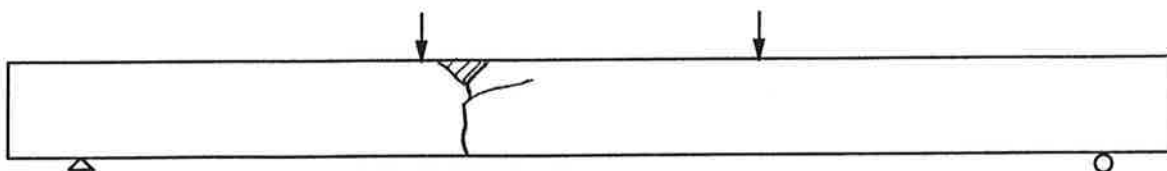
(b) fully-bonded beam with braided AFRP tendons



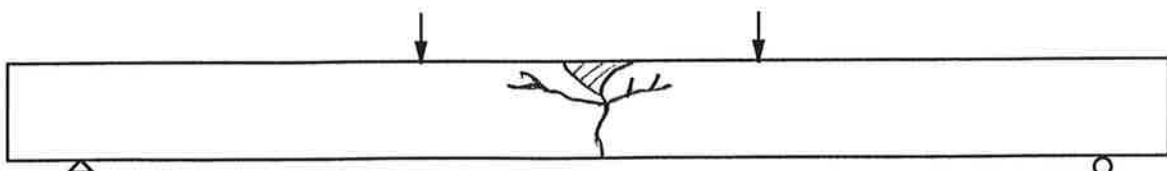
(c) fully-bonded beam with spiral wound AFRP tendons



(d) unbonded beam with steel tendons

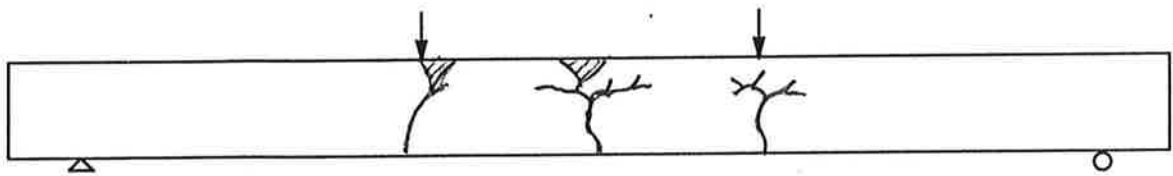


(e) unbonded beam with braided AFRP tendons

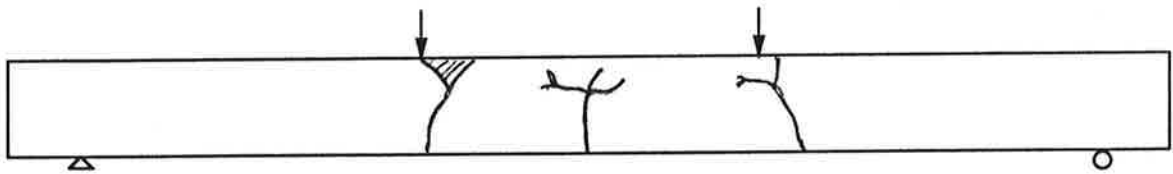


(f) unbonded beam with spiral wound AFRP tendons

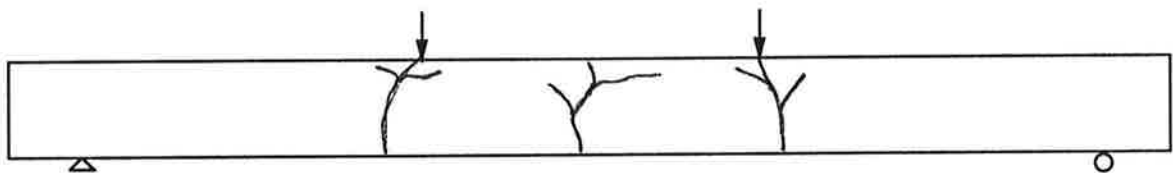
Figure 12 : Crack patterns - Fully-bonded and unbonded beams (schematic)



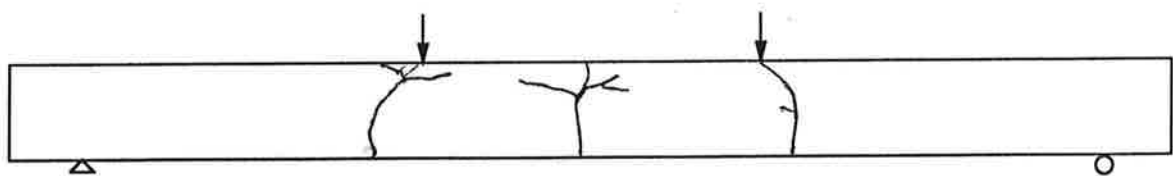
(a) intermittently-bonded 1 beam with braided AFRP tendons



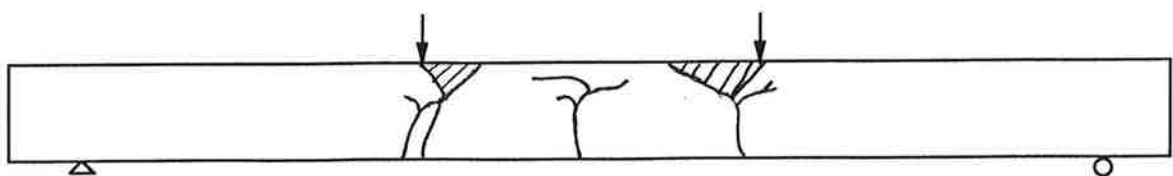
(b) intermittently-bonded 1 beam with spiral wound AFRP tendons



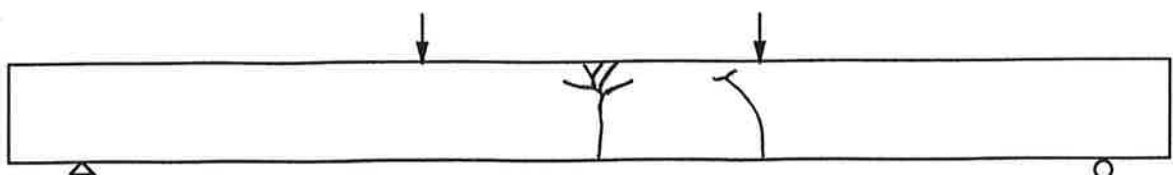
(c) intermittently-bonded 2 beam with braided AFRP tendons



(d) intermittently-bonded 2 beam with spiral wound AFRP tendons



(e) adhesive-bonded beam with braided AFRP tendons



(f) adhesive-bonded beam with spiral wound AFRP tendons

Figure 13: Crack patterns - Partially-bonded beams (schematic)

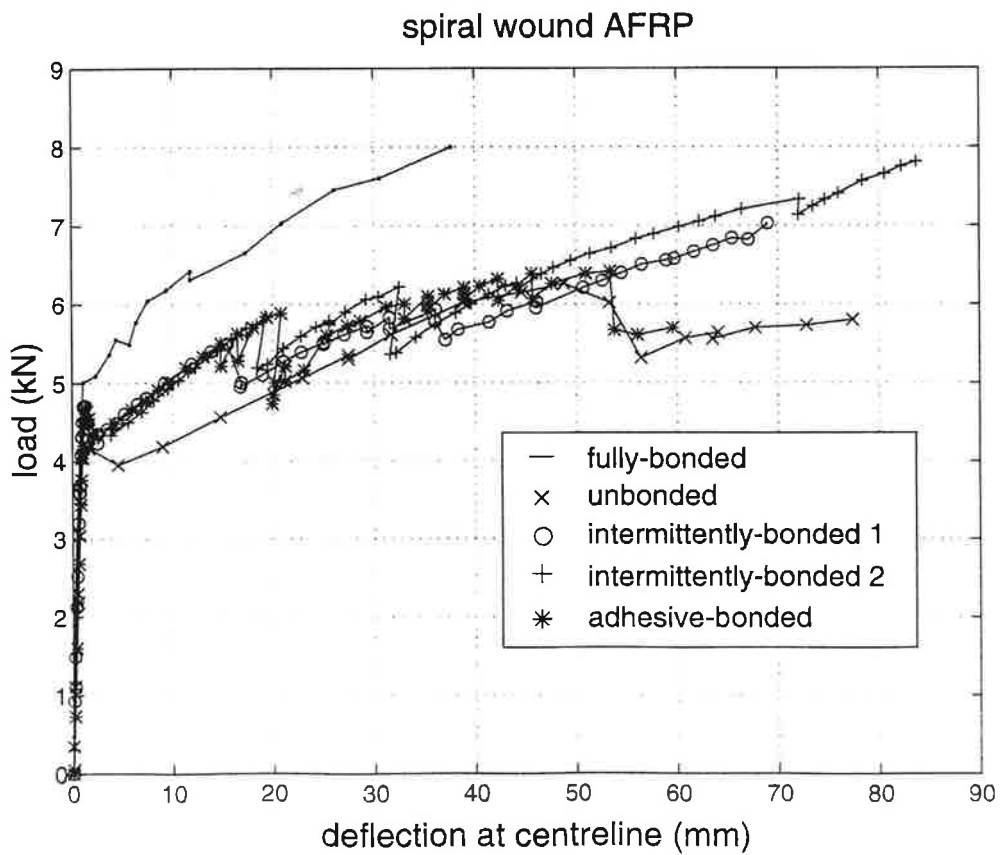
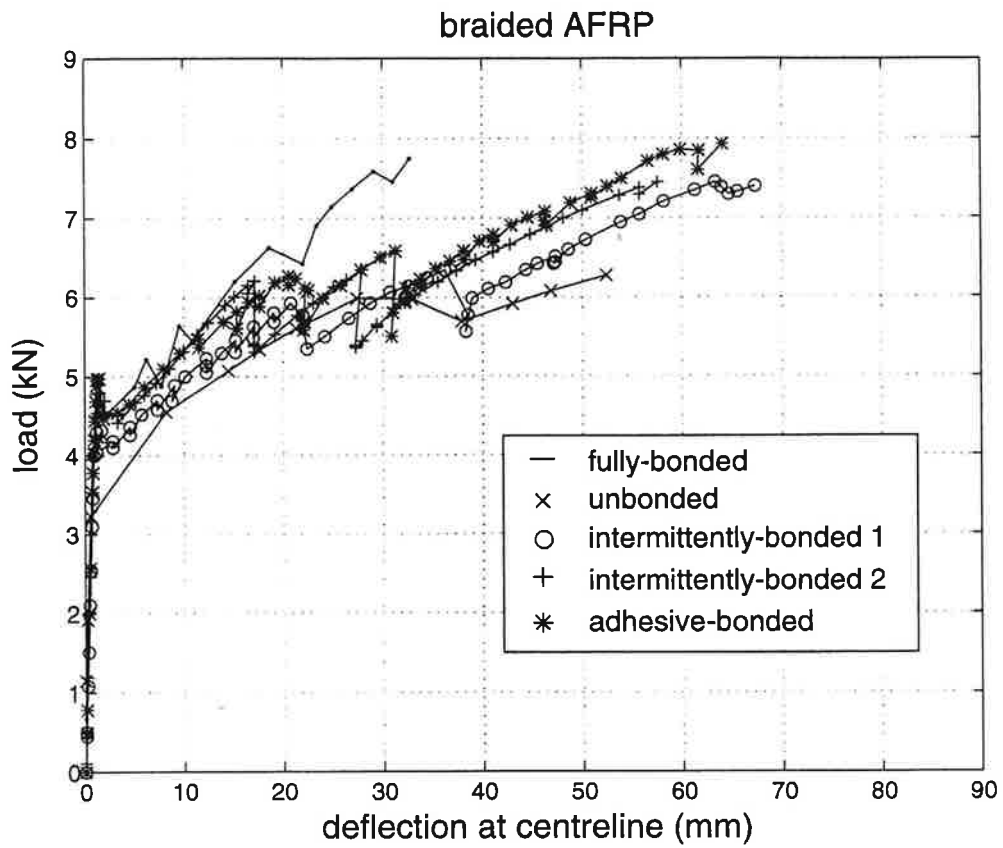


Figure 14 : Load-deflection curves for AFRP beams